BIOCHEMISTRY
including biophysical chemistry & molecular biology

ARTICLE

pubs.acs.org/biochemistry

Fluorescence Spectroscopy as a Probe of the Effect of Phosphorylation at Serine 40 of Tyrosine Hydroxylase on the Conformation of Its Regulatory Domain

Shanzhi Wang,[†] Mauricio Lasagna,[†] S. Colette Daubner,[‡] Gregory D. Reinhart,[†] and Paul F. Fitzpatrick*[,§]

[†]Department of Biochemistry and Biophysics, Texas A&M University, College Station, Texas 77843, United States

[‡]Department of Biology, St. Mary's University, San Antonio, Texas 78228, United States

[§]Department of Biochemistry and Center for Biomolecular Neuroscience, University of Texas Health Science Center, San Antonio, Texas 78229, United States

ABSTRACT: Phosphorylation of Ser40 in the regulatory domain of tyrosine hydroxylase activates the enzyme by increasing the rate constant for dissociation of inhibitory catecholamines from the active site by 3 orders of magnitude. To probe the changes in the structure of the N-terminal domain upon phosphorylation, individual phenylalanine residues at positions 14, 34, and 74 were replaced with tryptophan in a form of the protein in which the endogenous tryptophans had all been mutated to phenylalanine (W_3F TyrH). The steady-state fluorescence anisotropy of F74W W_3F TyrH was unaffected by phosphorylation, but the anisotropies of both F14W and F34W W_3F TyrH increased significantly upon phosphorylation. The fluorescence of the single tryptophan residue at position 74 was less readily quenched by acrylamide than those at the other two positions; fluorescence increased the rate constant for quenching of the residues at positions 14 and 34 but did not affect that for the residue at position 74. Frequency domain analyses were consistent with phosphorylation having no effect on the amplitude of the rotational motion of the indole ring at position 74, resulting in a small increase in the rotational motion of the residue at position 14 and resulting in a larger increase in the rotational motion of the residue at position 34. These results are consistent with the local environment at position 74 being unaffected by phosphorylation, that at position 34 becoming much more flexible upon phosphorylation, and that at position 14 becoming slightly more flexible upon phosphorylation. The results support a model in which phosphorylation at Ser40 at the N-terminus of the regulatory domain causes a conformational change to a more open conformation in which the N-terminus of the protein no longer inhibits dissociation of a bound catecholamine from the active site.

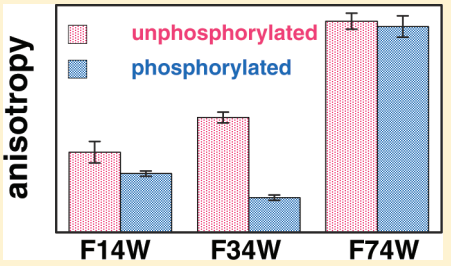

Tyrosine hydroxylase (TyrH) belongs to the non-heme iron-containing aromatic amino acid hydroxylase family, along with phenylalanine hydroxylase (PheH) and tryptophan hydroxylase.[1] The enzyme catalyzes the hydroxylation of tyrosine to dihydroxyphenylalanine (DOPA) using molecular oxygen and tetrahydrobiopterin (BH_4). As the first and rate-limiting enzyme in the biosynthesis of catecholamines, regulation of TyrH activity is critical. Feedback inhibition by catecholamines and activation by phosphorylation of Ser40 are the best established regulatory mechanisms.[2] As shown in Scheme 1, for TyrH to convert tyrosine into dihydroxyphenylalanine (DOPA), the active site iron must be ferrous.[3] However, the ferrous enzyme is readily oxidized to the ferric form,[4,5] rendering the enzyme inactive. The ferric enzyme can be reactivated by reduction, with BH_4 the most likely reductant.[5] Alternatively, a catecholamine can bind to the ferric iron in the active site. Dopamine, epinephrine, and norepinephrine all bind ferric TyrH with affinities of 1−5 nM.[6,7] The presence of a catecholamine bound to the iron prevents its reduction by BH_4, trapping the enzyme in an inactive form. This inhibition can be reversed upon phosphorylation of Ser40, which increases the catecholamine dissociation rate constant by 2−3 orders of magnitude.[6,7] As a result, the catecholamine can dissociate from the active site, allowing reduction to the active ferrous form.

The N-terminal ∼165 residues of TyrH constitute a regulatory domain that is required for tight binding of catecholamines but can be removed without significantly altering the enzyme activity.[8,9] However, the only available structures of TyrH are of an enzyme lacking these residues,[10] so that the structure of the regulatory domain is not known. Several lines of evidence indicate that the conformation of the regulatory domain is altered by catecholamine binding and by phosphorylation of Ser40. Peptide bonds near Ser40 become more susceptible to cleavage by trypsin upon phosphorylation and less sensitive when dopamine is bound.[11] Hydrogen−deuterium exchange mass spectrometry showed that upon dopamine binding residues 295−299 at the active site entrance and residues 35−71 in the regulatory domain are protected from exchange.[12] Phosphorylation of TyrH at Ser40 has the opposite effect on the exchange kinetics of residues 295−299, but residues 35−71 of the phosphorylated

Received: November 18, 2010
Revised: February 5, 2011
Published: February 08, 2011

Scheme 1

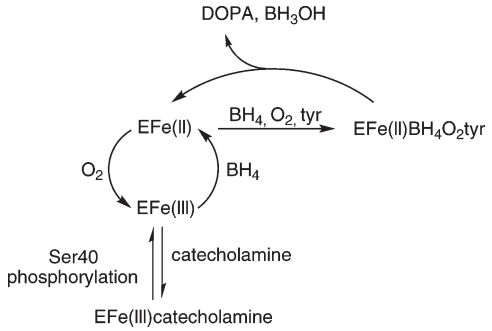

enzyme were not detectable by mass spectrometry.[12] These results led to the model that TyrH has a closed conformation, in which the regulatory domain of the enzyme extends across the active site, and an open conformation in which the active site is exposed. Dopamine in the active site would stabilize the closed conformation, while phosphorylation would favor the open form. The effects of dopamine on the deuterium incorporation kinetics of peptides in both the catalytic and regulatory domain support the existence of a closed conformation of the enzyme when a catecholamine is bound. However, the inability to detect by mass spectrometry peptides in the regulatory domain in the phosphorylated enzyme limited the conclusions that could be drawn about the structure and dynamics of the phosphorylated enzyme. To address this limitation, we have used fluorescence spectroscopy to probe changes in the dynamics and solvent accessibility of residues in the regulatory domain upon phosphorylation of Ser40. We have previously shown that mutating all three intrinsic tryptophans in TyrH to phenylalanines has little effect on enzyme activity or substrate binding.[13] We describe here the use of this tryptophan-free enzyme to study the effects of phosphorylation on the conformation of the N-terminus of TyrH.

EXPERIMENTAL PROCEDURES

Materials. HEPES (4-(2-hydroxyethyl)-1-piperazineethanesulfonic acid) was obtained from USB Co. (Cleveland, OH). Ultrapure glycerol and *N*-acetyl-L-tryptophanamide were from Sigma-Aldrich Chemical Co. (St. Louis, MO). All the other chemicals were of the highest purity commercially available.

Protein Purification. The plasmid for expression of mutant TyrH with the three intrinsic tryptophans replaced by phenylalanines has been described previously.[13] The introduction of a single tryptophan at position 14, 34, or 74 was performed by QuikChange site-directed mutagenesis (Stratagene). The purification of the mutant enzymes was modified from that described previously for wild-type TyrH.[14,15] After the heparin column, the enzymes were incubated with a 1.2 molar ratio of ferrous iron, followed by further purification with a Q-Sepharose column (10 × 200 mm).[12] Stoichiometric phosphorylation of TyrH by protein kinase A and purification of the phosphorylated enzymes were performed as previously described.[6,12] The purified protein was dialyzed into 50 mM HEPES, 100 mM KCl, and 10% ultrapure glycerol, pH 7.3, for the fluorescence experiments. Protein kinase A was purified from beef heart by the method of Flockhart and Corbin.[16]

Kinetic Assays. The enzyme activity was determined using a colorimetric end-point assay at pH 7 and 30 °C as previously described.[17] The dopamine dissociation rate constant was determined by monitoring the decrease in absorbance at 550 nm after the enzyme−dopamine complex was mixed with excess 2,3-dihydroxynaphthalene (DHN) at pH 7 and 10 °C as previously described.[6]

Fluorescence Analyses. The steady-state anisotropies and the effects of acrylamide on the tryptophan fluorescence were determined on an ISS Koala spectrofluorometer with a 300 W xenon lamp as the excitation source, using 2−5 μM enzyme in 50 mM HEPES, 10% glycerol, and 100 mM KCl at pH 7.0 and 22 °C. The emitted light was passed through a Schott WG-345 filter. For the anisotropy measurements, the samples were excited with vertically polarized light at 300 nm using a slit width of 4 nm. The emission intensities of both horizontally (I_H) and vertically (I_V) polarized light were measured, and the anisotropy (r) was calculated using eq 1.

$$r = (I_V - I_H)/(I_V + I_H) \quad (1)$$

For the quenching studies, samples in the presence of various acrylamide concentrations (Q) were excited at 300 nm, and the emission intensity (F) was measured. The data were analyzed using eq 2.

$$F_0/F = 1 + K_{SV}[Q] \quad (2)$$

Here, F_0 is the fluorescent intensity in the absence of acrylamide and K_{SV} is the Stern−Volmer constant.

Lifetime and dynamic anisotropy experiments were performed using an ISS K2 fluorometer with multifrequency phase and modulation as previously described.[13,18] The excitation light of 300 nm was generated from a light-emitting diode, and the emission at 345 nm was collected through a Schott WG-345 filter and a polarizer at an angle of 35° relative to the vertical laboratory axis. An *N*-acetyl-L-tryptophanamide solution was used as reference with a lifetime of 2.85 ns. Data were collected with modulation frequencies between 1 and 250 MHz. The calculations of the lifetimes were performed using a continuous Lorentzian distribution model, since it gave the best χ^2 value for all of the conditions, compared to models with one or two exponential decays or a Gaussian distribution.[20−22] Global analyses of the lifetime data and the dynamic anisotropy data, and the associated errors, were performed using Globals Unlimited software from the Laboratory for Fluorescence Dynamics, University of Illinois.

RESULTS

Activities of Single Tryptophan Enzymes. There are three tryptophan residues in TyrH, at positions 166, 233, and 372. Mutation of all three to phenylalanine yields a tryptophan-free enzyme (F_3 TyrH) with wild-type enzyme activity.[13] Three single tryptophan-containing enzymes were constructed by replacing each of the three aromatic amino acids in the regulatory domain of F_3 TyrH, Phe14, Phe34, and Phe74, with tryptophan, yielding F14W/F_3 TyrH, F34W/F_3 TyrH, and F74W/F_3 TyrH. The mutant enzymes have comparable k_{cat} and K_m values to wild-type TyrH (Table 1), suggesting that catalysis and substrate binding are not altered by the mutations. The dopamine dissociation rate constant was used as an indicator of the regulatory function of the mutants. Dopamine binds to TyrH to form a greenish complex, with an absorption maximum of 690 nm, whereas DHN binds to TyrH to form a complex with an absorption maximum of 550 nm. As a result, the increase of absorbance at 550 nm when a large excess of DHN is added to the

Table 1. Steady-State Kinetic Parameters and Dopamine Dissociation Rate Constants of TyrH Single Tryptophan Mutant Enzymes

				k_{off}[c] (s^{-1}) x 10^3	
enzyme	K_{PH4}[a] (μM)	K_{Tyr}[b] (μM)	k_{cat} (min^{-1})	unphosphorylated	phosphorylated
wild type	40 ± 4	40 ± 5	150 ± 14	0.0007[d]	0.87 ± 0.02
F14W/F_3	55 ± 8	24 ± 4	109 ± 4	<0.01	0.38 ± 0.02
F34W/F_3	77 ± 7	58 ± 4	121 ± 3	<0.01	0.39 ± 0.01
F74W/F_3	65 ± 7	43 ± 6	104 ± 4	<0.01	0.40 ± 0.01

[a] Conditions: 50 mM HEPES, pH 7, 1 mM dithiothreitol, 10 μM ferrous ammonium sulfate, 10 μg/mL catalase, and 100 μM tyrosine with 5−400 μM 6-$MePH_4$ at 25 °C. [b] Conditions: 50 mM HEPES, pH 7, 1 mM dithiothreitol, 10 μM ferrous ammonium sulfate, 10 μg/mL catalase, and 400 μM 6-$MePH_4$ with 5−400 μM tyrosine at 25 °C. [c] Conditions: 50 mM HEPES, pH 7, 100 mM KCl, 10% glycerol, ~30 μM enzyme, 45 μM dopamine, 30 μM DPTA, and 1 mM DHN at 10 °C. [d] From ref 32 at 15 °C.

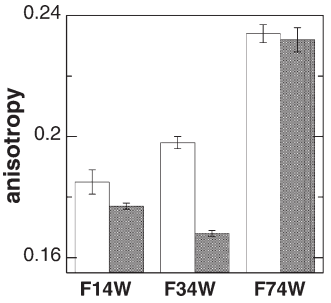

Figure 1. Effects of phosphorylation at Ser40 on the steady-state fluorescence anisotropy of the single tryptophans in TyrH mutant proteins. The white bars are for the unphosphorylated proteins, and the gray bars are for the phosphorylated proteins.

enzyme−dopamine complex can be used to measure the dopamine dissociation rate constant. Adding DHN to the dopamine complexes of the unphosphorylated mutant enzymes resulted in a slight increase in absorbance at 550 nm but no decrease in absorbance at longer wavelengths over 10 h, indicating that the mutants were slowly denaturing during the reaction. Still, these results allow us to set an upper limit on the dissociation rate constants for the unphosphorylated enzymes of 10^{-5} s^{-1}. Upon phosphorylation of the enzyme at Ser40, the dissociation rate constants for all three mutants increased to close to the value for wild-type TyrH (Table 1), establishing that the regulatory functions of the mutant enzymes are not compromised by the mutations.

Steady-State Anisotropy. The steady-state fluorescence anisotropy of the unique tryptophan residues in each of the three proteins was determined in order to probe the effect of phosphorylation on the local dynamics at each position. Figure 1 compares the steady-state anisotropies of the three single-tryptophan enzymes and shows the effects of phosphorylation on the anisotropies. If only the values for the unphosphorylated proteins are considered, the tryptophan residue in F74W/F_3 TyrH exhibits greater anisotropy than the tryptophan residues in the other two proteins, suggesting that residue 74 is in a more rigid local environment than the residues at positions 14 and 34. Phosphorylation of the enzyme has no effect on the anisotropy of F74W/F_3 TyrH, whereas the anisotropies of both F14W/F_3 TyrH and F34W/F_3 TyrH decrease significantly upon phosphorylation of Ser40. This is consistent with increased flexibility of the side chains at positions 14 and 34, with the largest effect on the residue closer to the phosphorylation site.

Frequency Domain Analyses. The multifrequency method,[19] in which the phase and modulation of the emitted light are measured as a function of the excitation frequency, was used to gain further insight into the dynamics of the indole side chains at positions 14, 34, and 74 and the effects of phosphorylation on the dynamics. The fluorescence lifetimes of the unique tryptophan residues in each of the three mutants were analyzed as continuous Lorentzian distributions with width W and central lifetime C (eq 3).[20−22] Alternative models utilizing either a single exponential decay or two exponential decays produced χ^2 values in the range of 200−400 and 9−15, respectively, and were therefore deemed to be inappropriate descriptions of the decay behavior. The values of these parameters for each of the single tryptophan mutant proteins are given in Table 2.

$$f(\tau) = \frac{A}{1 + \left(\frac{\tau - C}{W/2}\right)^2} \quad (3)$$

F14W/F_3 TyrH and F34W/F_3 TyrH have comparable lifetimes, while F74W/F_3 TyrH has a shorter lifetime. Upon phosphorylation of Ser 40, the lifetimes of both F14W/F_3 TyrH and F34W/F_3 TyrH increase by ~0.1 ns, while the lifetime of F74W/F_3 TyrH is unchanged. The lack of a significant change in these lifetimes upon phosphorylation is consistent with a recent study of the effects of phosphorylation of Ser40 on the fluorescence lifetime of tryptophan residues introduced into these positions in the isolated regulatory domain of human TyrH.[23]

To further quantify the rotational properties of each tryptophan and the effect of phosphorylation, the dynamic anisotropy of each was determined. The phase difference and modulation ratio of the emitted light as a function of the modulation frequency for each protein are shown in Figure 2. In the case of F14W/F_3 TyrH, the data in Figure 2C show that phosphorylation has no effect, consistent with the lack of an effect on the steady-state anisotropy. There is a small effect in the case of F74W/F_3 TyrH (Figure 2A), although an effect on the phase difference is only seen at the highest frequency. In contrast, phosphorylation resulted in a substantial change in both the phase difference and the modulation ratio for F34W/F_3 TyrH at all frequencies (Figure 2B). These results agree with the effects of phosphorylation on the steady-state anisotropies, in that the effect of phosphorylation on the dynamics is largest for the residue at position 34.

To gain quantitative insight into the dynamics of the individual tryptophan residues and the effects of phosphorylation, the data in Figure 2 were analyzed as a system in which the

Table 2. Effects of Phosphorylation on the Dynamics of TyrH Single Tryptophan Mutant Enzymes Determined from Frequency Domain Analyses

	lifetime						
enzyme[a]	center (ns)	width (ns)	χ^2	$r_0 - r_\infty$	θ_1 (ns)	χ^2	2ϕ (deg)[b]
F14W/F_3	3.26 ± 0.10	2.71 ± 0.08	2.1	0.060 ± 0.008	1.27 ± 0.15	2.1	53.2 ± 4.1
pF14W/F_3	3.40 ± 0.02	2.75 ± 0.04	1.5	0.069 ± 0.009	1.27 ± 0.15		57.7 ± 4.7
F34W/F_3	3.35 ± 0.09	3.36 ± 0.08	1.8	0.061 ± 0.002	1.00 ± 0.09	1.2	53.9 ± 1.1
pF34W/F3	3.46 ± 0.02	3.15 ± 0.04	2.3	0.080 ± 0.002	1.00 ± 0.09		63.3 ± 1.3
F74W/F_3	2.71 ± 0.05	2.05 ± 0.05	0.7	0.048 ± 0.007	1.62 ± 0.12	1.7	47.0 ± 3.7
pF74W/F_3	2.75 ± 0.02	2.14 ± 0.04	1.2	0.036 ± 0.006	1.62 ± 0.12		40.2 ± 3.6

[a] The lower case p in the front of the enzyme name designates the phosphorylated form. [b] Differential polarization data were fit to a model describing a hindered rotation with a slow global rotation using eq 4. The cone angle of the local rotation for the tryptophan was obtained from eq 5.

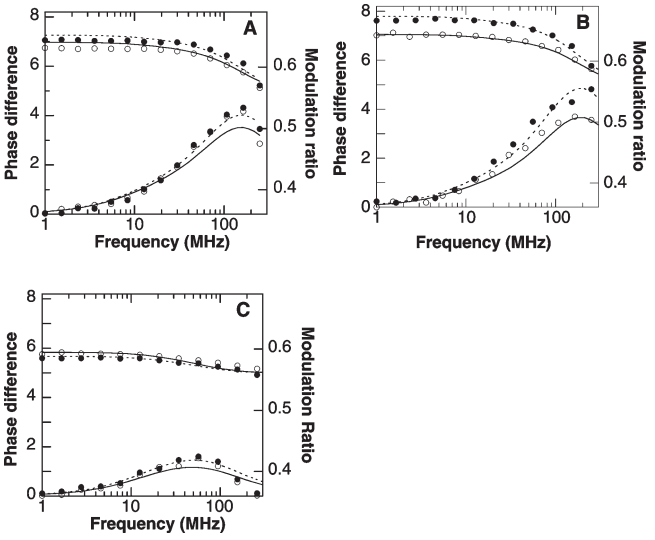

Figure 2. Effects of phosphorylation on the frequency dependence of the modulation ratio (upper lines) and phase difference (lower lines) of the single tryptophans in TyrH mutant proteins: (A) F14W/F_3 TyrH; (B) F34W/F_3 TyrH; (C) F74W/F_3 TyrH. The open symbols are for the unphosphorylated enzymes, and the solid symbols are for the enzymes phosphorylated at Ser40.

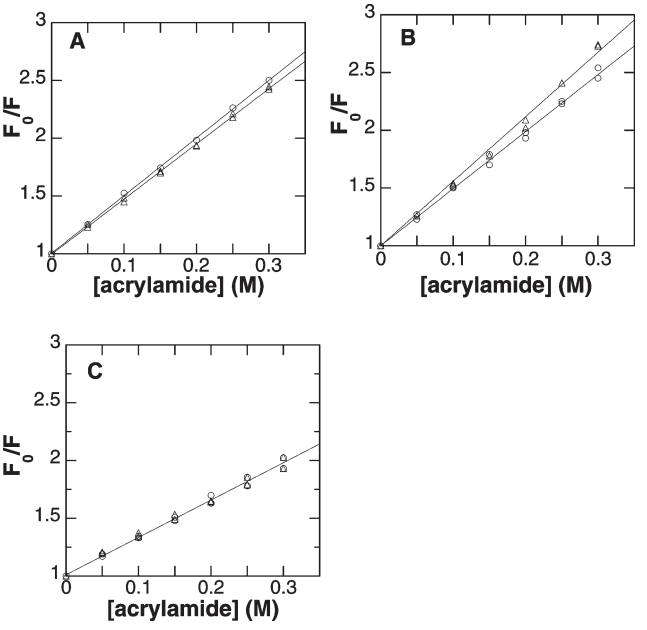

Figure 3. Effect of phosphorylation at Ser40 on the acrylamide quenching of the fluorescence of the single tryptophans in TyrH mutant proteins: (A) F14W/F_3 TyrH; (B) F34W/F_3 TyrH; (C) F74W/F_3 TyrH. The circles are the data for the unphosphorylated enzymes, and the diamonds are the data for the phosphorylated enzymes.

fluorophore experiences a global rotation plus a hindered local rotation, using eq 4.[24,25]

$$r(t) = (r_0 - r_\infty)e^{-t/\theta_1} + r_\infty e^{-t/\theta_2} \quad (4)$$

Here, r_0 is the anisotropy at time zero and is independent of the rotational motion, r_∞ is the anisotropy persisting after a relatively long time ($t \gg \theta_1$), and θ_1 and θ_2 are the local and global rotational correlation times ($\theta_1 \ll \theta_2$). Thus, r_∞ and $r_0 - r_\infty$ are the contributions (i.e., amplitudes) of the slow global rotation and the faster local rotation, respectively, to the anisotropy. The value of θ_2, which reflects the motion of the entire protein, was fixed at 115 ns based on our earlier study of the fluorescence properties of TyrH.[13] When the data for the phosphorylated and unphosphorylated forms of each mutant enzyme were analyzed individually, the resulting values of r_0 and θ_1 were independent of the phosphorylation status for each mutant protein. Consequently, a global analysis of the data was performed for each mutant protein, combining the data for the phosphorylated and unphosphorylated forms and assigning the same r_0 and θ_1 irrespective of the phosphorylation status. The analyses yielded the same r_0 value of 0.21 ± 0.01 for all three proteins, but different θ_1 and r_∞ values for the individual mutants (Table 2). There is a clear effect of phosphorylation on the $r_0 - r_\infty$ value for F34W/F_3 TyrH. The other two proteins show smaller changes with somewhat larger errors. These larger errors likely reflect an inability to fit the data due to the limitations of describing the rotational behavior of the two mutants with only one global rotation component and one local hindered rotation component. However, using models with more local hindered rotations to fit the data did not significantly improve the fitting. Visual inspection of the data in Figure 3 suggests that the errors in the $r_0 - r_\infty$ value for F74W/F_3 TyrH reflect the difficulty of fitting the low sensitivity of the phase difference and modulation ratio of the tryptophan residue in this protein to the frequency and that there is no change in the value upon phosphorylation at Ser40. In contrast, there may be small effects of phosphorylation on the parameters of the single tryptophan residue in F14W/F_3 TyrH.

The lack of an effect of phosphorylation on either of the local or global rotational correlation times for the different mutant proteins suggests that the changes in $r_0 - r_\infty$ upon

Table 3. Effects of Phosphorylation on the Quenching by Acrylamide of the Fluorescence of TyrH Single Tryptophan Mutant Enzymes

enzyme	K_{SV} (M^{-1})	k_q (M^{-1} ns^{-1})
F14W/F_3	5.01 ± 0.03	1.53 ± 0.05
pF14W/F_3[a]	4.76 ± 0.02	1.40 ± 0.01
F34W/F_3	4.94 ± 0.05	1.47 ± 0.04
pF34W/F3	5.59 ± 0.08	1.62 ± 0.02
F74W/F_3	3.28 ± 0.04	1.21 ± 0.02
pF74W/F_3	3.30 ± 0.05	1.20 ± 0.02

[a] The lower case p in the front of the enzyme name designates the phosphorylated form.

phosphorylation reflect changes in the amplitude of the rotation available to the indole ring at position 34 and possibly at position 14. This amplitude can be described as a cone angle associated with the local motion, using eq 5.

$$\cos(\phi) = \frac{1}{2}\sqrt{1 + 8\sqrt{\frac{r_\infty}{r_0}} - 1} \quad (5)$$

The individual cone angles are given in Table 3. For both F14W/F_3 TyrH and F34W/F_3 TyrH, phosphorylation results in an increase in the amplitude of the local motion as reflected in the cone angle. In contrast, there is a decrease in the cone angle for F74W/F_3 TyrH; this likely reflects the uncertainty in the data as discussed above.

Fluorescence Quenching with Acrylamide. Acrylamide quenching of the fluorescence of the individual indole rings in the three single tryptophan mutant enzymes was used as an additional probe of the changes in local structure upon phosphorylation. The results are shown as Stern−Volmer plots in Figure 3. The values of the Stern−Volmer quenching constants (K_{SV}) for the mutant enzymes were determined from eq 2 and are given in Table 3. The fluorescence of the tryptophan at position 74 is much less sensitive to quenching by acrylamide than are those at positions 14 and 34. In addition, phosphorylation of the enzyme does not affect the sensitivity of F74W/F_3 TyrH fluorescence to acrylamide. In contrast, the sensitivities of the two more N-terminal residues to quenching are altered by phosphorylation, with an increase of 12% in the K_{SV} value for F34W/F_3 TyrH and a smaller decrease (~5%) in the K_{SV} value for F14W/F_3 TyrH.

The relationship between the Stern−Volmer quenching constant and the quenching rate constant k_q is given by eq 6, where τ is the lifetime of the fluorophore.

$$K_{SV} = k_q\tau \quad (6)$$

The center values of the Lorentzian lifetime distributions determined above were used to convert the K_{SV} values to the quenching rate constants. These k_q values are listed in Table 3. The differences in the k_q values among the three tryptophan locations and the changes upon phosphorylation parallel the K_{SV} values, consistent with the relatively small changes in the lifetimes. The tryptophan side chain at position 74 is less accessible to quenching, and the accessibility of this residue does not change when Ser40 is phosphorylated. In contrast, phosphorylation of Ser40 alters the k_q values of the tryptophan indole rings at positions 14 and 34, but in opposite directions. In the unphosphorylated enzyme, the k_q values for F14W/F_3 TyrH and F34W/F_3 TyrH are comparable. Upon phosphorylation, the k_q value of F14W/F_3 TyrH decreases by about 8%, while the k_q value of F34W/F_3 TyrH increases by ~10%. This suggests that phosphorylation increases the solvent exposure of the indole ring of the tryptophan at position 34, the closest one to the phosphorylation site, but decreases the exposure of the side chain at position 14.

DISCUSSION

The lack of any structural model of the regulatory domain of TyrH has limited the understanding of the structural changes associated with regulatory phenomena that modulate the activity of the enzyme. Indeed, structural analysis of the regulatory domains of all three of the aromatic amino acid hydroxylases has proved difficult. While numerous structures have been described for PheH, there is only one report describing a structure that includes the regulatory domain.[26] Similarly, the only structures available of tryptophan hydroxylase lack the regulatory domain.[27,28] The dramatic effect of phosphorylation of Ser40 on the rate constants for dissociation of catecholamines bound in the active site of TyrH[6,7] establishes that there must be a physical linkage between this region of the regulatory domain and the active site of that enzyme. The changes in the kinetics of deuterium exchange into the peptide bonds of TyrH upon dopamine binding provided strong support for a model in which the enzyme can exist in a conformation in which residues around Ser40 in the N-terminal regulatory domain extend across the active site and that dopamine bound in the active site stabilizes this conformation.[12] However, those data did not provide as much support for the hypothesis that phosphorylation alters the protein conformation to one in which the active site is exposed, allowing the catecholamine to dissociate. While the exchange studies did establish that phosphorylation and dopamine binding have opposite effects on the accessibility of residues at the active site opening, the inability to analyze peptides around Ser40 in the phosphorylated enzyme precluded any definitive conclusions regarding the structure or dynamics of the N-terminus in the enzyme phosphorylated at Ser40. The three most N-terminal aromatic residues in TyrH, Phe14, Phe34, and Phe74, are appropriately placed to probe the structural change in the regulatory domain upon phosphorylation. The deuterium exchange studies established that the peptide containing Phe74 does not change conformation significantly upon phosphorylation. Phe34 provides a probe close to the phosphorylation site that compensates for the lack of information regarding this region of the protein. Phe14 is positioned appropriately for a probe close to the N-terminus in a region that was not analyzed in the deuterium exchange studies. Replacement of each of these residues with tryptophan in the context of our mutant construct lacking any tryptophan residues thus provided enzymes in which structural changes important to the effects of phosphorylation could be analyzed. The lack of any significant effect of introduction of a single tryptophan at position 14, 34, or 74 on either the activity or the effect of phosphorylation of Ser40 on dopamine binding establishes that the relatively conservative replacement of phenylalanine by tryptophan did not in itself significantly disrupt the protein structure.

The combined results of the effects of phosphorylation on the acrylamide quenching, steady-state anisotropy, and frequency-domain fluorescence parameters of F14W/F_3, F34W/F_3, and F74W/F_3 TyrH establish that phosphorylation of Ser40 alters

the structure of the regulatory domain significantly around residue 34, close to the phosphorylation site, slightly alters the structure at the more N-terminal residue 14, and does not affect the structure around the more C-terminal residue 74. This is consistent with a model in which phosphorylation of Ser40 alters the conformation of the N-terminal portion of the regulatory domain to a more open form by disrupting interactions between residues around the phosphorylation site and the catalytic domain.

The quenching rate constants for the individual single tryptophan mutant proteins suggest that all three positions are relatively exposed on the protein surface.[29] In the absence of a structure of TyrH that includes the regulatory domain, the structure of rat PheH containing both the regulatory and catalytic domains[26] serves as the best model. As noted above, that structure shows the N-terminal 33 residues of the regulatory domain extending across the surface of the catalytic domain and hindering access to the active site. The N-terminal domain of rat TyrH is larger than the N-terminal domain of PheH, and the first 34 residues of phenylalanine hydroxylase show no significant similarities to the N-terminal residues of TyrH. However, the subsequent residues, 83−164 of TyrH, align relatively well with residues 35−117 of PheH, with the only insertions or deletions occurring at loops in the PheH structure and 31 (38%) of the residues being identical or conservative replacements. These residues in PheH form a globular ATC domain[30] that contains a regulatory binding site for phenylalanine.[31] While there is no evidence that the regulatory domain of TyrH binds amino acids, the similarities of these regions of the two proteins support a model in which the regulatory domain of TyrH is composed of a C-terminal ATC-like domain and the N-terminal ~80 residues extend across the surface of the catalytic domain. The accessibility of the single tryptophan residues at positions 14, 34, and 74 supports such a model. Among these three residues, that at position 74 has the lowest k_q value, suggesting it is somewhat more buried. Phosphorylation of Ser40 has no effect on the k_q value for the tryptophan at this position, suggesting that the local environment around the side chain is not altered upon phosphorylation. This is consistent with the lack of an effect of phosphorylation on the kinetics of deuterium incorporation into peptide 75−83.[12] The k_q values for the other two positions are essentially identical in the unphosphorylated enzyme, consistent with similar solvent accessibilities of the side chains at positions 14 and 34. The peptide bonds of peptides 28−34 and 35−41 completely exchange their protons with deuterium from solvent within 7 s in the unphosphorylated enzyme, providing further evidence that this region of the protein is accessible to solvent. No peptide containing residues before Ala28 was detected by mass spectrometry in that analysis. The increase in the k_q value of the tryptophan residue at position 34 upon phosphorylation establishes that the side chain at this position becomes more accessible to solvent when Ser40 is phosphorylated, supporting a model in which phosphorylation shifts TyrH to a more open conformation in which the N-terminal residues no longer prevent access to the active site. The single tryptophan at position 14 appears to be less solvent accessible upon phosphorylation based on the change in the k_q value. The small size of the change in the K_{SV} value for F14W/F_3 TyrH upon phosphorylation suggests that any change in the environment at this position is quite small.

The effects of phosphorylation on the steady-state and dynamic anisotropy support the conclusions drawn from the quenching analysis and provide further information regarding the local structural changes. The data in Figure 1 establish that phosphorylation has no detectable effect on the local motion of the indole side chain at position 74 but results in a significant increase in the local motion of the residue at position 34 and a lesser increase at position 14. These changes can be described as increases in the amplitudes of the motions of the side chains as measured by the cone angles. The similar cone angles for unphosphorylated F14W/F_3 and F34W/F_3 TyrH provide a rationale for their similar k_q values. The increase in the cone angle for F34W/F_3 TyrH upon phosphorylation provides further support for the conclusion that phosphorylation of Ser40 alters the conformation of the regulatory domain so that this region is more accessible. The small increase in the cone angle for F14W/F_3 TyrH upon phosphorylation is opposite that expected from the effect of phosphorylation on the k_q value but consistent with only a small change in the local environment at this position. The smaller cone angle for F74W/F_3 TyrH suggests that the side chain at this position is in a slightly more restricted environment than is the case for the residues at the other two positions. The apparent decrease in the cone angle for this protein upon phosphorylation can be attributed to inaccuracies in modeling the small changes in modulation and phase change for this position.

In conclusion, the fluorescence properties of the three single tryptophan mutants of TyrH provide further insight into the structural effects of Ser40 phosphorylation on the regulatory domain of the enzyme. The results show that the region near residue 34 has substantially greater flexibility upon phosphorylation, the region near residue 14 becomes slightly more accessible, and that near residue 74 does not undergo structural rearrangement upon phosphorylation. This is consistent with TyrH existing in open and closed conformations, with the equilibrium between them being affected by the key regulatory controls of phosphorylation at Ser40 and catecholamine binding.

AUTHOR INFORMATION

Corresponding Author

*E-mail: fitzpatrick@biochem.uthscsa.edu. Phone: 210-567-8264. Fax: 210-567-8778.

Funding Sources

This work was supported by NIH Grant R01 GM047291 to P.F. F. and NIH Grant R01 GM033216 to G.D.R.

ABBREVIATIONS

TyrH, tyrosine hydroxylase; F_3 TyrH, W166F/W233F/W372F TyrH; PheH, phenylalanine hydroxylase; BH_4, tetrahydrobiopterin; DOPA, 3,4-dihydroxyphenylalanine; DHN, 2,3-dihydroxynaphthalene.

REFERENCES

(1) Fitzpatrick, P. F. (1999) The tetrahydropterin-dependent amino acid hydroxylases. *Annu. Rev. Biochem. 68*, 355–381.

(2) Dunkley, P. R., Bobrovskaya, L., Graham, M. E., Von Nagy-Felsobuki, E. I., and Dickson, P. W. (2004) Tyrosine hydroxylase phosphorylation: regulation and consequences. *J. Neurochem. 91*, 1025–1043.

(3) Fitzpatrick, P. F. (1989) The metal requirement of rat tyrosine hydroxylase. *Biochem. Biophys. Res. Commun. 161*, 211–215.

(4) Ramsey, A. J., Hillas, P. J., and Fitzpatrick, P. F. (1996) Characterization of the active site iron in tyrosine hydroxylase—Redox states of the iron. *J. Biol. Chem. 271*, 24395–24400.

(5) Frantom, P. A., Seravalli, J., Ragsdale, S. W., and Fitzpatrick, P. F. (2006) Reduction and oxidation of the active site iron in tyrosine hydroxylase: Kinetics and specificity. *Biochemistry 45*, 2372–2379.

(6) Ramsey, A. J., and Fitzpatrick, P. F. (1998) Effects of phosphorylation of serine 40 of tyrosine hydroxylase on binding of catecholamines: Evidence for a novel regulatory mechanism. *Biochemistry 37* 8980–8986.

(7) Ramsey, A. J., and Fitzpatrick, P. F. (2000) Effects of phosphorylation on binding of catecholamines to tyrosine hydroxylase: Specificity and thermodynamics. *Biochemistry 39*, 773–778.

(8) Daubner, S. C., Lohse, D. L., and Fitzpatrick, P. F. (1993) Expression and characterization of catalytic and regulatory domains of rat tyrosine hydroxylase. *Protein Sci. 2*, 1452–1460.

(9) Wang, S. (2010) Identification of structural changes related to the regulation of tyrosine hydroxylase, 107 pp, Ph.D. Thesis, Texas A&M University, College Station, TX.

(10) Goodwill, K. E., Sabatier, C., Marks, C., Raag, R., Fitzpatrick, P. F., and Stevens, R. C. (1997) Crystal structure of tyrosine hydroxylase at 2.3 Ångstrom and its implications for inherited neurodegenerative diseases. *Nat. Struct. Biol. 4*, 578–585.

(11) McCulloch, R. I., and Fitzpatrick, P. F. (1999) Limited proteolysis of tyrosine hydroxylase identifies residues 33−50 as conformationally sensitive to phosphorylation state and dopamine binding. *Arch. Biochem. Biophys. 367*, 143–145.

(12) Wang, S., Sura, G. R., Dangott, L. J., and Fitzpatrick, P. F. (2009) Identification by hydrogen/deuterium exchange of structural changes in tyrosine hydroxylase associated with regulation. *Biochemistry 48*, 4972–4979.

(13) Sura, G. R., Lasagna, M., Gawandi, V., Reinhart, G. D., and Fitzpatrick, P. F. (2006) Effects of ligands on the mobility of an active-site loop in tyrosine hydroxylase as monitored by fluorescence anisotropy. *Biochemistry 45*, 9632–9638.

(14) Daubner, S. C., and Fitzpatrick, P. F. (1999) Site-directed mutants of charged residues in the active site of tyrosine hydroxylase. *Biochemistry 38*, 4448–4454.

(15) Daubner, S. C., Hillas, P. J., and Fitzpatrick, P. F. (1997) Characterization of chimeric pterin-dependent hydroxylases: Contributions of the regulatory domains of tyrosine and phenylalanine hydroxylase to substrate specificity. *Biochemistry 36*, 11574–11582.

(16) Flockhart, D. A., and Corbin, J. D. (1984) Preparation of the catalytic subunit of cAMP-dependent protein kinase, in *Brain Receptor Methodologies, Part A* (Maranos, P. J., Campbell, I. C., and Cohen, R. M., Eds.) pp 209−215, Academic Press, New York.

(17) Fitzpatrick, P. F. (1991) The steady state kinetic mechanism of rat tyrosine hydroxylase. *Biochemistry 30*, 3658–3662.

(18) Johnson, J. L., West, J. K., Nelson, A. D. L., and Reinhart, G. D. (2007) Resolving the fluorescence response of *Escherichia coli* carbamoyl phosphate synthetase: Mapping intra- and intersubunit conformational changes. *Biochemistry 46*, 387–397.

(19) Gratton, E., Jameson, D. M., and Hall, R. D. (1984) Multifrequency phase and modulation fluorometry. *Annu. Rev. Biophys. Bioeng. 13*, 105–124.

(20) Alcala, J. R., Gratton, E., and Prendergast, F. G. (1987) Resolvability of fluorescence lifetime distributions using phase fluorometry. *Biophys. J. 51*, 587–596.

(21) Alcala, J. R., Gratton, E., and Prendergast, F. G. (1987) Interpretation of fluorescence decays in proteins using continuous lifetime distributions. *Biophys. J. 51*, 925–936.

(22) Alcala, J. R., Gratton, E., and Prendergast, F. G. (1987) Fluorescence lifetime distributions in proteins. *Biophys. J. 51* 597–604.

(23) Obsilova, V., Nedbalkova, E., Silhan, J., Boura, E., Herman, P., Vecer, J., Sulc, M., Teisinger, J., Dyda, F., and Obsil, T. (2008) The 14-3-3 protein affects the conformation of the regulatory domain of human tyrosine hydroxylase. *Biochemistry 47*, 1768–1777.

(24) Munro, I., Pecht, I., and Stryer, L. (1979) Subnanosecond motions of tryptophan residues in proteins. *Proc. Natl. Acad. Sci. U.S.A. 76*, 56–60.

(25) Lipari, G., and Szabo, A. (1980) Effect of librational motion on fluorescence depolarization and nuclear magnetic resonance relaxation in macromolecules and membranes. *Biophys. J. 30*, 489–506.

(26) Kobe, B., Jennings, I. G., House, C. M., Michell, B. J., Goodwill, K. E., Santarsiero, B. D., Stevens, R. C., Cotton, R. G. H., and Kemp, B. E. (1999) Structural basis of intrasteric and allosteric controls of phenylalanine hydroxylase. *Nat. Struct. Biol. 6*, 442–448.

(27) Windahl, M. S., Petersen, C. R., Christensen, H. E., and Harris, P. (2008) Crystal structure of tryptophan hydroxylase with bound amino acid substrate. *Biochemistry 47*, 12087–12094.

(28) Wang, L., Erlandsen, H., Haavik, J., Knappskog, P. M., and Stevens, R. C. (2002) Three-dimensional structure of human tryptophan hydroxylase and its implications for the biosynthesis of the neurotransmitters serotonin and melatonin. *Biochemistry 41*, 12569–12574.

(29) Lakowicz, J. R. (1999) *Principles of Fluorescence Spectroscopy*, 2nd ed., Kluwer Academic, New York.

(30) Grant, G. A. (2006) The ACT domain: A small molecule binding domain and its role as a common regulatory element. *J. Biol. Chem. 281*, 33825–33829.

(31) Li, J., Ilangovan, U., Daubner, S. C., Hinck, A. P., and Fitzpatrick, P. F. (2011) Direct evidence for a phenylalanine site in the regulatory domain of phenylalanine hydroxylase, *Arch. Biochem. Biophys. 505*, 250−255

(32) McCulloch, R. I., Daubner, S. C., and Fitzpatrick, P. F. (2001) Effects of substitution at serine 40 of tyrosine hydroxylase on catecholamine binding. *Biochemistry 40*, 7273–7278.